Supplementary Information

Supplementary Materials and Methods

Cell culture. Wild type and NPC1-null (CT43) Chinese hamster ovary (CHO) fibroblasts were maintained in DMEM-Ham's F-12 medium (50-50 mix) supplemented with 10% FCS, L-glutamine, and penicillin–streptomycin. Vero African grivet monkey kidney cells and 293T human embryonic kidney cells were maintained in DMEM supplemented with 10% FCS, L-glutamine, and penicillin–streptomycin. VH-2 viper heart cells (ATCC) were cultured in MEM supplemented with 10% FCS and penicillin-streptomycin at 29°C. All mammalian cell lines were maintained in a humidified 5% CO_2 incubator.

NPC1 and NPC1L1 constructs. Human NPC1 and NPC1L1 cDNAs were ligated in-frame to a triple flag sequence, and the resulting genes encoding C-terminally FLAG-tagged NPC1 and NPC1L1 proteins were subcloned into the *BamHI* and *SalI* restriction sites of the pBABE-puro retroviral vector (Morgenstern and Land, 1990). Constructs encoding flag-tagged NPC1 'loop-minus' mutants in pBABE-puro [ΔA, lacking NPC1 amino acid residues 24-252); ΔC, lacking residues 381-611); ΔI, (lacking residues 865-1088)] were generated by replacing the indicated sequence with a *BglII* restriction site. To engineer the individual loop domain constructs, a cassette vector encoding the following sequence elements was first generated and cloned into the *BamHI* and *SalI* sites of pBABE-puro: NPC1 signal peptide (encoding NPC1 amino acid residues 1-24), *MluI* restriction site, the first NPC1 transmembrane domain (residues 267-295), NPC1 C-tail (residues 1252-1278), gly-gly-gly-ser linker, and triple flag tag. Each loop domain (A, residues 25-266; C, residues 373-620; I, residues 854-1098) was cloned into the *MluI* site of this cassette vector. Vectors expressing domain C-flag and domain C-flag^{tailless} differ in only one respect: the latter lacks the NPC1 C-tail sequence. All constructs were verified by automated DNA sequencing.

VH-2 and CT43 cell populations stably expressing NPC1 proteins. For transduction of VH-2 cells, the full-length human NPC1 cDNA (Origene) was cloned into the retroviral vector pMXsIRESblasti-FLAG (Carette et al., 2011). For transduction of CHO WT and CT43 cells, the pBABE-puro-based retroviral vectors described above were used. Retroviruses packaging the transgenes were produced by

triple transfection in 293T cells, and target cells were directly exposed to sterile-filtered retrovirus-laden supernatants in the presence of polybrene (6 μg/mL). Transduced cell populations were selected with blasticidin (20 μg/mL; for pMX) or puromycin (10 μg/mL; for pBABE-puro).

Expression of NPC1 proteins by transient transfection. 293T cells were transfected with pBABE-puro constructs encoding WT or mutant NPC1 or NPC1L1 proteins using polyethyleneimine (PEI), as described previously (Dube et al., 2009). At 48 h post-transfection, cells were lysed as described below to generate extracts for GP-NPC1 binding assays.

NPC1-containing cell extracts for GP-NPC1 binding assays. CT43 or 293T cells expessing WT or mutant NPC1 or NPC1L1 proteins were washed with PBS, and packed cell pellets were lysed by incubation at 4˚C with NTE-CHAPS buffer (pH 7.5) or MES-EDTA-CHAPS buffer (pH 5.1) (10 mM 2-(N-morpholino)ethanesulfonic acid, 140 mM NaCl, 1 mM EDTA, 0.5% vol/vol 3-[(3-cholamidopropyl)dimethylammonio]-1-propanesulfonate)) supplemented with a protease inhibitor cocktail (Roche). Typically, 1 mL buffer was used to lyse 2×10^7 cell-equivalents. To promote cell lysis, cell suspensions were probe-sonicated (lowest setting, 5 pulses of 5 sec each) in an ice-water bath. Lysates were cleared by centrifugation at 14,000 ×g for 10 min, and supernatants were used immediately.

Affinity purification of NPC1-flag. CT43 cells expressing NPC1-flag (2×10^8 cells) were harvested and lysed as above, and the extracts were incubated with magnetic beads coated with anti-flag antibody (0.25 mL) at 4˚C with mixing for 12-16 h. Beads were then extensively washed with NTE-CHAPS, and bound proteins were eluted with 10 packed-bead volumes of triple flag peptide (5 mg/mL; Sigma). The eluate was concentrated and buffer-exchanged using a centrifugal concentrator (100 kDa molecular weight cutoff; Pall Biosciences), and NPC1-flag purity was assessed by SDS-PAGE and staining with the Krypton infrared protein-binding dye (Thermo).

Recombinant VSV displaying NPC1 domain C-VSV G chimera (rVSV-domain C). A VSV genome plasmid in which the VSV glycoprotein G open-reading frame had been replaced with an *MluI*-

NotI restriction cassette (pVSVΔG-eGFP-MN) (Whelan et al., 1995; Wong et al., 2010) was engineered to express NPC1 domain C-flag in the VSV G position as follows. The VSV G signal peptide sequence (encoding G amino acid residues 1-16) was fused in-frame to NPC1 domain C (encoding NPC1 amino acid residues 373-620), the VSV G transmembrane domain (last 71 residues of G), and a flag tag sequence. This chimeric domain C construct was cloned into the *MluI* and *NotI* sites of pVSVΔG-eGFP-MN. Recombinant virus was recovered and amplified as described previously (Whelan et al., 1995). A final amplification in cells lacking the complementing VSV G plasmid was performed in order to obtain virus particles only expressing the domain C-VSV G chimera. Viral incorporation of this protein was confirmed by SDS-PAGE and immunoblotting (Fig. S5a).

Generation and purification of soluble domain C and GPΔTM proteins. A construct engineered to encode NPC1 domain C (residues 372-622) flanked by sequences that form a stable, antiparallel coiled coil, and fused to a preprotrypsin signal sequence and flag and hexahistidine tags at its N–terminus has been described (Deffieu and Pfeffer, 2011). A plasmid encoding EBOV GPΔTM (residues 1-650) fused to a hexahistidine tag at the C–terminus was kindly provided by G.G. Olinger (USAMRIID). Soluble domain C was expressed in human 293-Freestyle cells (Invitrogen) and purified from conditioned supernatants by nickel affinity chromatography, as described previously (Deffieu and Pfeffer, 2011). GPΔTM was expressed in 293-EBNA cells (ATCC) and purified from conditioned supernatants in a similar manner.

Neutralization of rVSV-GP-EBOV by rVSV-domain C. Uncleaved or cleaved rVSV-GP-EBOV particles were mixed with rVSV-bald or rVSV-domain C for for 30 min at 4°C. Subsequently, the virus mixtures were deposited onto carbon-coated copper grids and stained with 2% phosphotungstic acid (PTA) in H_2O (pH 7.5). Virus particles were viewed using a Tecnai G^2 Spirit BioTWIN transmission electron microscope (FEI, Hillsboro, OR). In parallel, virus mixtures were exposed to WT CHO monolayers in dark 96-well clear-bottom plates at an MOI of 0.01. After 7 h at 37°C, eGFP expression was quantified with a Typhoon 9400 imager (GE Healthcare).

Neutralization of rVSV-GP-EBOV by soluble domain C. Uncleaved or cleaved rVSV-GP-EBOV particles were mixed with soluble domain C for 1 h at room temp. Subsequently, the virus mixtures were diluted and exposed to Vero cell monolayers for 1 h at 37˚C, at which time NH_4Cl (20 mM) was added to block additional entry events and cell-to-cell spread. Viral infectivity was determined at 12-16 h post-infection by enumerating eGFP-positive cells.

Authentic filoviruses and infections. Cells were exposed to EBOV-Zaire 1995 (Jahrling et al., 1999) or MARV-Ci67 (Swenson et al., 2008) at an MOI of 3 for 1 h. Viral inoculum was then removed and fresh culture media was added. At 48 h post-infection, cells were fixed with formalin, and blocked with 1% bovine serum albumin. EBOV-infected cells and uninfected controls were incubated with EBOV GP-specific monoclonal antibodies 13F6 (Wilson et al., 2000) or KZ52 (Maruyama et al., 1999)**.** MARV-infected cells and uninfected controls were incubated with MARV GP-specific monoclonal antibody 9G4 (Swenson et al., 2004). Cells were washed with PBS prior to incubation with either goat anti-mouse IgG or goat anti-human IgG conjugated to Alexa 488. Cells were counterstained with Hoechst stain (Invitrogen), washed with PBS and stored at 4°C. Infected cells were quantitated by fluorescence microscopy and automated image analysis. Images were acquired at 9 fields/well with a 10× objective lens on a Discovery-1 high content imager (Molecular Devices) or at 6 fields/well with a 20× objective lens on an Operetta (Perkin Elmer) high content device. Discovery-1 images were analyzed with the "live/dead" module in MetaXpress software. Operetta images were analyzed with a customized scheme built from image analysis functions present in Harmony software.

EBOV virus-like particles (VLPs). eGFP-labeled EBOV VLPs were generated by co-transfection of an eGFP-VP40 matrix fusion protein and EBOV GP and concentrated by ultracentrifugation, as described previously (Martin-Serrano et al., 2004). In vitro-cleaved VLPs were generated by thermolysin digestion as described for VSV-GP in Materials and Methods.

Assay for VLP attachment to cells. Cells in 6-well plates were exposed to uncleaved or thermolysin-cleaved VLPs (5 μL/well) in cell culture medium (1 mL/well total), and centrifuged at 2500 rpm and 4°C

for 10 min. Cells were then washed, collected by gentle scraping, resuspended in PBS containing 2% FCS, and analyzed for eGFP-positive cells by flow cytometry.

VSV M-release assay. Cells grown on 12-mm coverslips coated with poly-D-lysine (Sigma-Aldrich) were pre-treated with cycloheximide (20 μg/mL) for 30 min to arrest cellular protein synthesis, and then inoculated with rVSV at an MOI of 200 in the presence of cycloheximide. After 3 h, cells were washed with PBS and fixed with 2% paraformaldehyde for 15 min at room temperature. To detect incoming VSV M protein, fixed cells were incubated with the monoclonal antibody 23H12 (Lefrancois and Lyles, 1982) ,followed by incubation with an Alexa 594-conjugated goat anti-mouse secondary antibody. Cells were counter-stained with DAPI to visualize nuclei, washed, and mounted onto glass slides. M localization images were acquired by fluorescence microscopy.

Confocal fluorescence microscopy. CHO cells grown on 12-mm coverslips were either directly fixed or transfected with a plasmid expressing the late endosomal/lysosomal marker LAMP1-eGFP using Lipofectamine 2000 transfection reagent (Invitrogen). Cells were processed for imaging the next day. In addition, VH-2 control cells and VH-2 cells stably expressing human NPC1-flag were inoculated with a MOI of 300 of Alexa-647-labelled rVSV-GP-EBOV (Carette et al., 2011). At the indicated time-points, cells were washed with an acid buffer to remove surface-bound virus. All cells were fixed in 4% paraformaldehyde for 15 min at room temperature. Where indicated, cells were stained with Alexa 594-conjugated wheat germ agglutinin (WGA; Invitrogen) in PBS for 5 min at room temperature to outline the plasma membrane. The quantification of viral particles (total fluorescence/cell in arbitrary units) in VH-2 cells was performed with ImageJ software (n=10 per condition).

For antibody stainings, cells were permeabilized with 0.1% Triton X-100 for 5 min at room temp, blocked overnight with PBS containing 1% BSA, and incubated with an anti-flag antibody (Sigma-Aldrich) or an anti-NPC1 antibody (Novus Biologicals). Bound primary antibodies were detected by incubation with Alexa 488- or Alexa 594-conjugated secondary antibodies (Invitrogen). Cells were mounted onto glass slides using ProLong antifade (Invitrogen) and images were acquired using a spinning disk confocal microscope (Zeiss) with a 63x objective (Cureton et al., 2010). Image analysis was performed with

Slidebook 4.2 software (Intelligent Imaging Innovations).

Cell-surface biotinylation. Monolayers of CT43 cells expressing NPC1 domain C-flag or domain C-flag^{tailless} were washed with ice-cold PBS containing 0.1% glucose (PBSG) and exposed to EZ-Link NHS-PEG4-biotin in PBSG (5 mM; Thermo) for 1 h at 4˚C. Unreacted reagent was quenched by extensive washing with PBSG containing NH_4Cl (50 mM), and cells were lysed with ice-cold NTE-CHAPS buffer supplemented with a protease inhibitor cocktail, as described above. Cell lysates were cleared by centrifugation at 14,000 ×g for 10 min. In parallel, CHAPS extracts of unlabeled cells were biotinylated as above to generate a 'total lysate labeling' control. Flag-tagged proteins in the cell extracts were retrieved by immunoprecipitation with flag antibody-coated beads as described in Materials and Methods ('GP-NPC1 co-immunoprecipitation assays' section). Captured proteins were subjected to SDS-PAGE and immunoblotting with streptavidin-horseradish peroxidase and anti-flag antibody to detect biotinylated and flag-tagged proteins, respectively.

Supplementary References

Carette, J.E., Raaben, M., Wong, A.C., Herbert, A.S., Obernosterer, G., Mulherkar, N., Kuehne, A.I., Kranzusch, P.J., Griffin, A.M., Ruthel, G., *et al.* Ebola virus entry requires the cholesterol transporter Niemann-Pick C1. *Nature*, doi:10.1038/nature10348.

Cureton, D.K., Massol, R.H., Whelan, S.P., and Kirchhausen, T. (2010). The length of vesicular stomatitis virus particles dictates a need for actin assembly during clathrin-dependent endocytosis. *PLoS Pathog* **6**, e1001127.

Deffieu, M. and Pfeffer, S.R. (2011). Niemann-Pick type C1 function requires lumenal domain residues that mediate cholesterol-dependent NPC2 binding. *Proc Natl Acad Sci USA* **108**, 18932-18936.

Dube, D., Brecher, M.B., Delos, S.E., Rose, S.C., Park, E.W., Schornberg, K.L., Kuhn, J.H., and White, J.M. (2009). The primed ebolavirus glycoprotein (19-kilodalton GP1,2): sequence and residues critical for host cell binding. *J Virol* **83**, 2883-2891.

Jahrling, P.B., Geisbert, T.W., Geisbert, J.B., Swearengen, J.R., Bray, M., Jaax, N.K., Huggins, J.W., LeDuc, J.W., and Peters, C.J. (1999). Evaluation of immune globulin and recombinant interferon-alpha2b for treatment of experimental Ebola virus infections. *J Infect Dis* **179 Suppl 1**, S224-234.

Kwon, H.J., Abi-Mosleh, L., Wang, M.L., Deisenhofer, J., Goldstein, J.L., Brown, M.S., and Infante, R.E. (2009). Structure of N-terminal domain of NPC1 reveals distinct subdomains for binding and transfer of cholesterol. Cell *137*, 1213-1224.

Lee, J.E., Fusco, M.L., Hessell, A.J., Oswald, W.B., Burton, D.R., and Saphire, E.O. (2008). Structure of the Ebola virus glycoprotein bound to an antibody from a human survivor. Nature **454**, 177-182.

Lefrancois, L. and Lyles D.S. (1982). The interaction of antibody with the major surface glycoprotein of vesicular stomatitis virus. I. Analysis of neutralizing epitopes with monoclonal antibodies. *Virology* **121**, 157-167.

Martin-Serrano, J., Perez-Caballero, D., and Bieniasz, P.D. (2004). Context-dependent effects of L domains and ubiquitination on viral budding. J. Virol. *78*, 5554-5563.

Maruyama, T., Rodriguez, L.L., Jahrling, P.B., Sanchez, A., Khan, A.S., Nichol, S.T., Peters, C.J., Parren, P.W., and Burton, D.R. (1999). Ebola virus can be effectively neutralized by antibody produced in natural human infection. *J Virol* **73**, 6024-6030.

Morgenstern, J.P., and Land, H. (1990). Advanced mammalian gene transfer: high titre retroviral vectors with multiple drug selection markers and a complementary helper-free packaging cell line. *Nucleic Acids Res* **18**, 3587-3596.

Swenson, D.L., Warfield, K.L., Larsen, T., Alves, D.A., Coberley, S.S., and Bavari, S. (2008). Monovalent virus-like particle vaccine protects guinea pigs and nonhuman primates against infection with multiple Marburg viruses. *Expert Rev Vaccines* **7**, 417-429.

Weissenhorn, W., Carfi, A., Lee, K.H., Skehel, J.J., and Wiley, D.C. (1998). Crystal structure of the Ebola virus membrane fusion subunit, GP2, from the envelope glycoprotein ectodomain. Mol. Cell *2*, 605-616.

Whelan, S.P., Ball, L.A., Barr, J.N., and Wertz, G.T. (1995). Efficient recovery of infectious vesicular stomatitis virus entirely from cDNA clones. *Proc Natl Acad Sci USA* **92**, 8388-8392.

Wilson, J.A., Hevey, M., Bakken, R., Guest, S., Bray, M., Schmaljohn, A.L., and Hart, M.K. (2000). Epitopes involved in antibody-mediated protection from Ebola virus. Science *287*, 1664-1666.

Wong, A.C., Sandesara, R.G., Mulherkar, N., Whelan, S.P., and Chandran, K. (2010). A forward genetic strategy reveals destabilizing mutations in the Ebolavirus glycoprotein that alter its protease dependence during cell entry. *J Virol* **84**, 163-175.

Supplementary Figure Legends

Fig. S1. Hypothesized structural rearrangements in the Ebola virus glycoprotein during viral entry, and a topological model of the Niemann-Pick C1 protein. (a) Surface-shaded views of EBOV GP in its pre-fusion (PDB id: 3CSY (Lee et al., 2008)) and putative post-fusion conformations (PDB id: 1EBO (Weissenhorn et al., 1998)) are shown. C–terminal GP2 sequences were not visualized in 1EBO and are modeled. EBOV GP is a trimer of GP1-GP2 heterodimers. GP1 consists of four structural subdomains, the base, the head, which contains the putative receptor-binding site (rbs), the glycan cap, and the mucin domain (modeled). GP is cleaved by endosomal cysteine proteases during entry to generate GP_{CL}, which lacks the glycan cap and mucin subdomains and contains an exposed rbs. GP_{CL} rearranges in response to an unknown fusion trigger, resulting in GP1-GP2 dissociation, insertion of the GP2 fusion loops into the target membrane, and finally, the formation of the'six-helix bundle' GP2 configuration. These conformational changes drive viral membrane fusion. The disposition of GP1 in $GP_{post\text{-}fusion}$ is unknown. (b) Topological model of NPC1 based on Davies and Ioannou (2000). Domain A contains a sterol-binding domain, but the specific functions of domains C and I are unknown (Kwon et al., 2009). In the present studies, a flag epitope tag was appended to the C–terminus of NPC1.

Fig. S2. The NPC1-dependent filovirus entry block in VH-2 viper heart cells is at a late entry step and is not caused by a deficiency in endo/lysosomal cholesterol transport. (a) Control and human NPC1 (hNPC1)-expressing VH-2 cells were exposed to Alexa 647-labeled rVSV-GP-EBOV-eGFP. At 8 h post-infection, the cells were fixed after an acid wash to remove cell surface-bound virus. Cells were stained with Alexa 594-conjugated wheat germ aggluttinin (WGA) to outline the plasma membrane and WGA (red), internalized viral particles (blue), and virus-expressed eGFP (green) were visualized by confocal fluorescence microscopy. (b) Viral particles internalized into cells from panel a were quantitated with ImageJ software (total fluorescence/cell in arbitrary units; n=10 cells per condition). Greater numbers of perinuclear viral puncta were observed in the control VH-2 cells than in the human NPC1-expressing cells, suggesting that viral particles undergo attachment, internalization, and delivery to late endosomal compartments, but cannot escape from these compartments in the absence of human NPC1. (c) VH-2 cells

were transfected with human NPC1-flag and infected with Alexa 647-labeled rVSV-GP-EBOV-eGFP at 48 h after transfection as described above. At 8 h post-infection, cells were fixed and stained with an anti-flag antibody. Colocalization of NPC1-flag and internalized viral particles was visualized by confocal fluorescence microscopy. The inlay represents a 12× digital zoom of the boxed area in the main image. Viral particles were readily observed inside NPC1-flag-positive vesicles (arrows). (d) Control and human NPC1-expressing VH-2 cells were left untreated or exposed to the NPC1 pathway inhibitor U18666A (20 μM) for 24 h. Cells were then stained with the fluorescent cholesterol-binding dye, filipin. Intracellular cholesterol accumulation was visualized by fluorescence microscopy. Scale bar, 10 μm. Profound cholesterol storage was observed only upon U18666A treatment, indicating that these cells possess a functional pathway for egress of cholesterol from endo/lysosomal compartments.

Fig. S3. Cellular localization of NPC1 'loop-minus' mutants lacking luminal domains A, C, or I.. Late endosomal/lysosomal localization of NPC1 proteins stably expressed in CHO CT43 cells was assessed by confocal fluorescence microscopy. Cells were transfected to express a LAMP1-eGFP fusion protein, fixed, and then immunostained for NPC1 with an anti-flag antibody. The bottom right image in each quadrant represents a 15× digital zoom of the boxed area in each overlay image. All of the mutant NPC1 proteins showed substantial colocalization with LAMP1-eGFP (white arrowheads).

Fig. S4. Expression and cellular localization of synthetic membrane proteins containing individual NPC1 luminal domains A, C, or I. (a) CT43 CHO cells stably expressing domain A-flag, domain C-flag, domain I-flag, or domain C-flag^{tailless} were lysed and subjected to SDS-PAGE, and expression of each protein was assessed by immunoblotting (IB) with an anti-flag antibody. Cellular cyclin-dependent kinase 4 (CDK4) was used as a loading control. M_r, relative molecular weight. Samples for detection of each type of protein were resolved on the same gel. (b) Late endosomal/lysosomal localization of domain A-flag, domain C-flag, domain I-flag, and domain C-flag^{tailless} was assessed by confocal fluorescence microscopy as described in Fig. S3. The bottom right image in each quadrant represents a 15× digital zoom of the boxed area in each overlay image. Domain A-flag and domain C-flag showed substantial colocalization with LAMP1-eGFP (white arrowheads), but domain I-flag did not, and its filamentous distribution was consistent with

its retention in the ER.

Fig. S5. Recombinant VSV displaying a NPC1 domain C-VSV G chimera clusters virus containing cleaved but not uncleaved filovirus glycoproteins. (a) rVSV-domain C particles incorporate NPC1 domain C. Cell supernatants containing rVSV-G, rVSV-bald (lacking a virus-encoded surface glycoprotein), and rVSV-domain C were concentrated by ultracentrifugation and subjected to immunoblotting with anti-flag antibody. Samples were resolved on the same gel. (b) Capacity of rVSV-domain C to bind to rVSV-GP. rVSV-GP and rVSV-GP_{CL} were preincubated with rVSV-domain C or rVSV-bald. Virus mixtures were stained with phosphotungstic acid and visualized by transmission electron microscopy. Arrows indicate large clusters of viral particles. This is a larger version of the image in Fig. 5b, and is shown for clarity.

Fig. S6. Purified forms of soluble GP and NPC1 domain C. Purified preparations of EBOV GP lacking the transmembrane domain (GPΔTM) and soluble domain C were resolved on SDS-polyacrylamide gels and visualized with the Krypton protein stain (Thermo). Samples were resolved on the same gel.

Fig. S7. Expression of NPC1 in WT CHO cells. CHO cells stably expressing a control vector or human NPC1-flag were lysed and subjected to SDS-PAGE. Expression of endogenous NPC1 and ectopic NPC1-flag was assessed by immunoblotting (IB) with anti-NPC1 and anti-flag antibodies, respectively. Samples for detection of each epitope were resolved on the same gel.

Fig. S8. A GP mutant defective at NPC1 binding can mediate viral attachment to cells that is not enhanced by NPC1 overexpression. WT CHO cells expressing endogenous levels of NPC1 or overexpressing NPC1-flag (see Fig. S7) were exposed to EBOV virus-like particles bearing GP(WT) or GP(3Ala) at 4˚C for 30 min and binding was assessed by flow cytometry. Flow histograms were gated for eGFP positivity (mean fluorescence intensity>10), and this analysis gate was used to quantitate % eGFP-positive cells in Fig. 7e.

Fig. S9. A GP2 fusion-loop mutant virus binds to NPC1. (a) Uncleaved and cleaved VSV-GP(F535R) were

incubated with cell extracts containing NPC1-flag, and GP(F535R) was retrieved by immunoprecipitation (IP) with monoclonal antibody KZ52. NPC1-flag in immune pellets and supernatants was detected by immunoblotting (IB) with an anti-flag antibody. Pellets and supernatants were resolved on separate gels (one gel for each) but exposed simultaneously to the same piece of film. (b) GP pre-fusion structure [PDB id: 3CSY (Lee et al., 2008)] with GP1 (blue) and GP2 (green) in surface-shaded and cartoon representations, respectively. GP2 fusion loop residue F535 (purple) is shown as balls-and-sticks. GP1 residues critical for NPC1-binding (K114+K115+K140) and that contact each GP2 fusion loop are highlighted in red and yellow, respectively. Residue F88, which falls into both categories, is shown in orange.

Fig. S10. Retargeting of a synthetic NPC1 domain C-based receptor to the plasma membrane. (*a*) Plasma membrane localization of WT NPC1-flag, domain C-flag, and domain C-flag^{tailless} in CT43 cells was assessed by confocal fluorescence microscopy. Cells were exposed to Alexa 594-conjugated wheat germ aggluttinin (WGA) to outline the plasma membrane, and then fixed and immunostained for NPC1 with an anti-flag antibody. The bottom right image in each quadrant represents a 15× digital zoom of the boxed area in each overlay image. Only domain C-flag^{tailless} localizes extensively to the plasma membrane (white arrows). (b) Detection of domain C at the plasma membrane by cell-surface biotinylation. Intact CT43 cells expressing domain C-flag and domain C-flag^{tailless} or extracts derived from these cells were exposed to an amine-specific biotinylation probe, NHS4-PEG-biotin, at 4˚C. Cells were then lysed, and flag-tagged proteins were recovered by immunoprecipitation (IP) with an anti-flag antibody. Immune pellets were subjected to SDS-PAGE and immunoblotting with streptavidin and an anti-flag antibody to detect biotinylated and flag-tagged proteins, respectively. Samples for detection of each epitope were resolved on the same gel (one gel each for streptavidin a nd flag). Only domain C-flag^{tailless} was labeled by the cell-surface biotinylation reagent.

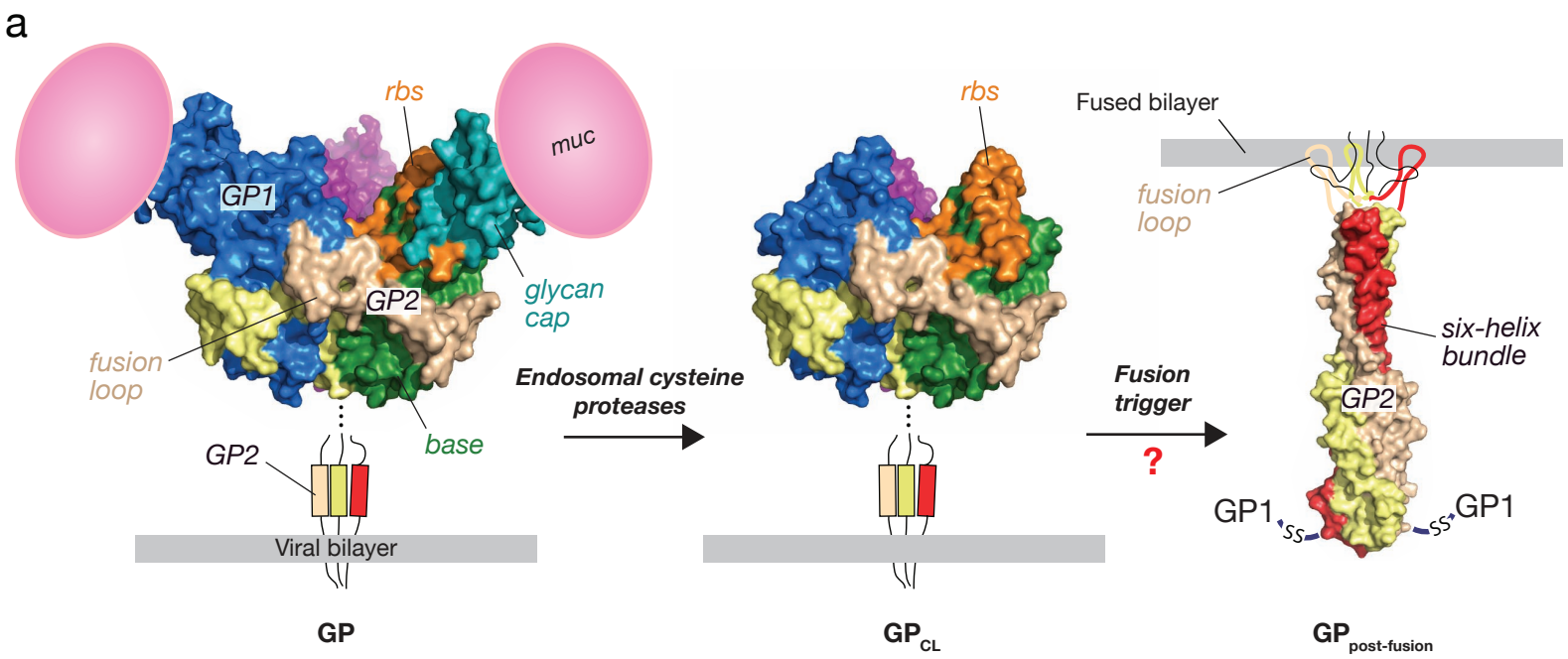
a
rbs
muc
GP1
GP2
glycan cap
fusion loop
base
GP2
Viral bilayer
GP
Endosomal cysteine proteases
rbs
GP$_{CL}$
Fusion trigger
?
Fused bilayer
fusion loop
six-helix bundle
GP2
GP1
SS
SS
GP1
GP$_{post-fusion}$

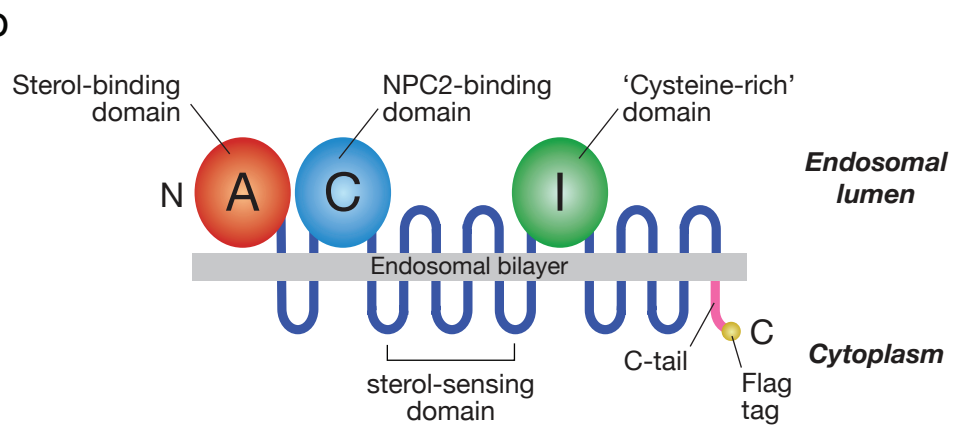
b
Sterol-binding domain
NPC2-binding domain
'Cysteine-rich' domain
N
A
C
I
Endosomal lumen
Endosomal bilayer
C
C-tail
Cytoplasm
sterol-sensing domain
Flag tag

a

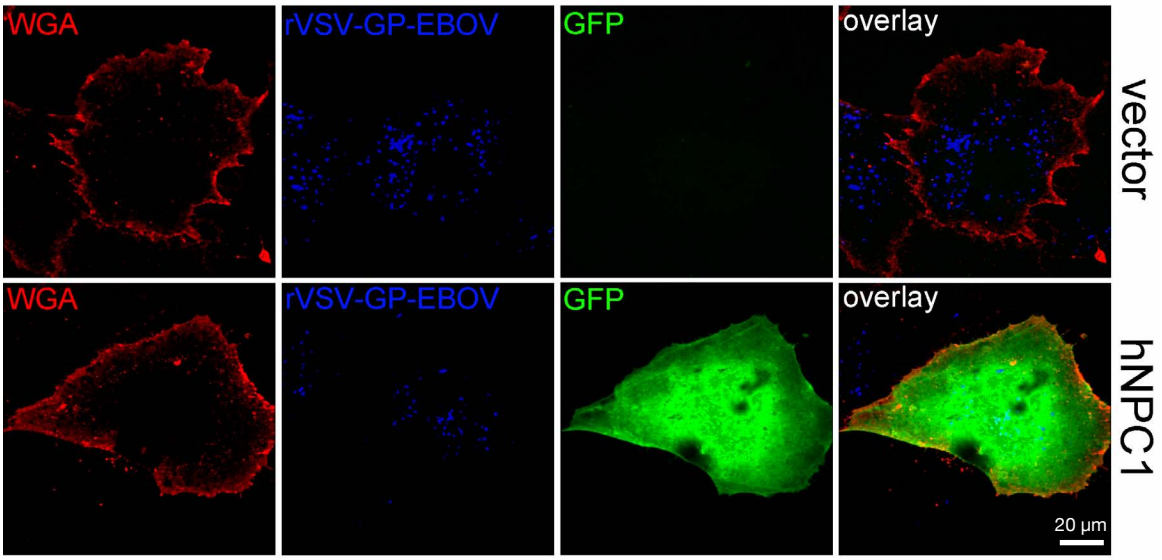

b

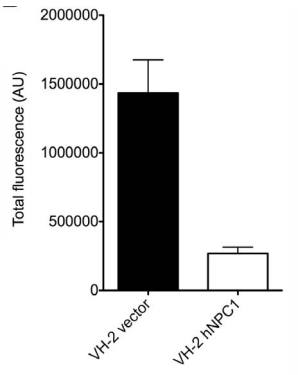

c

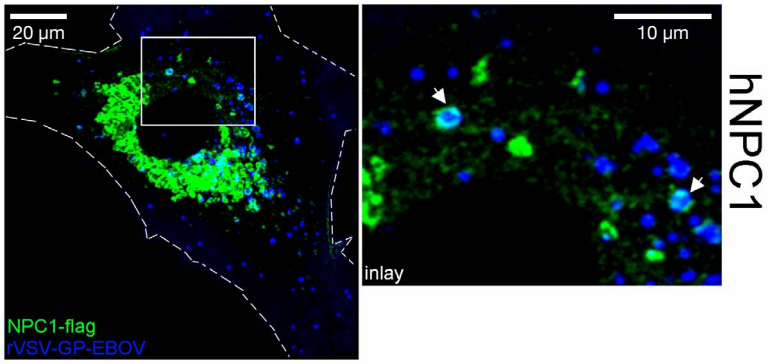

d

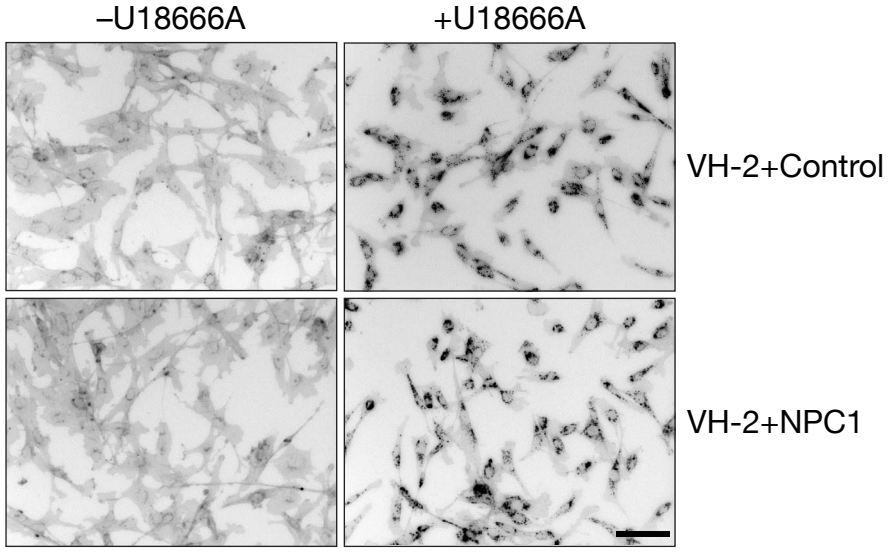

Filipin staining

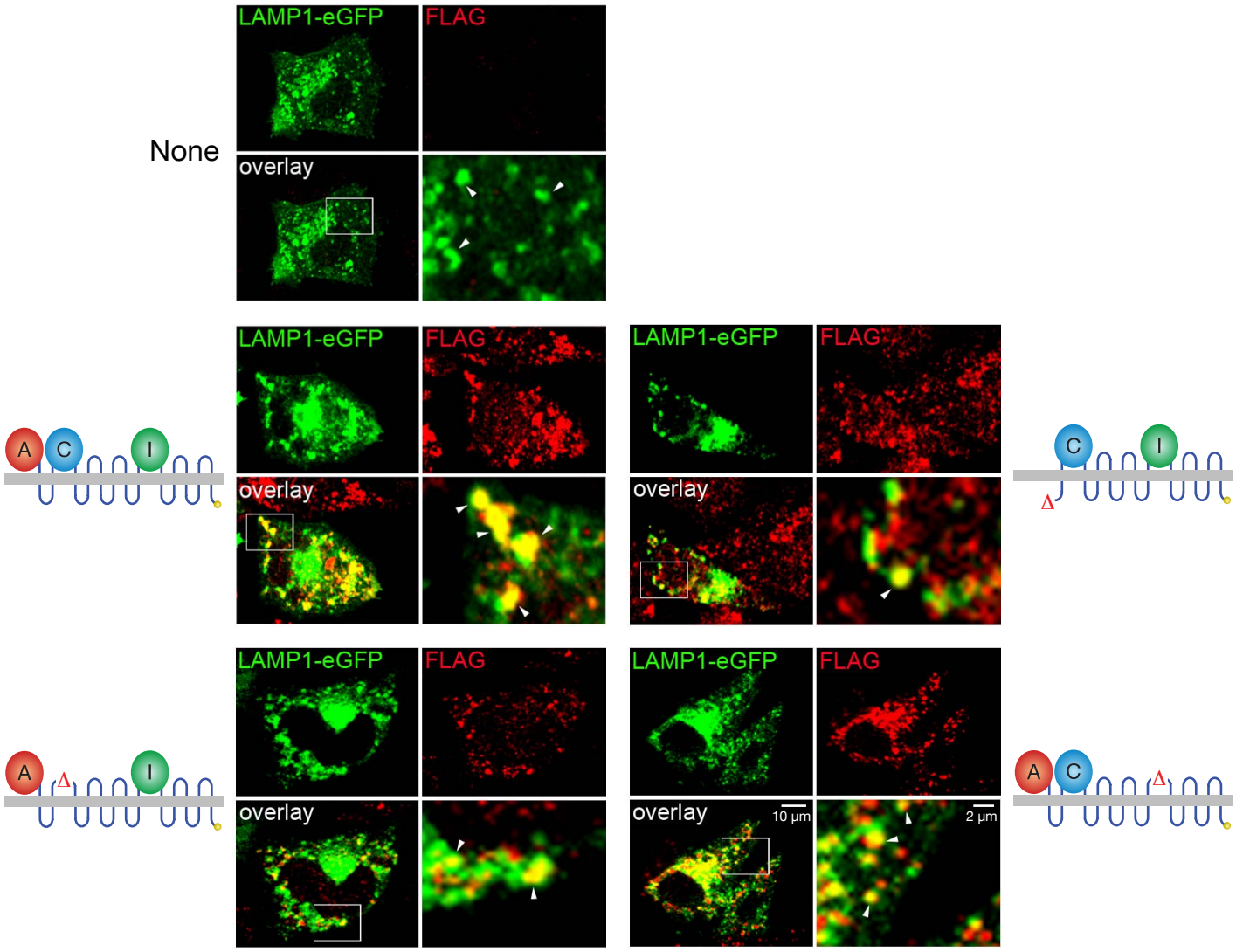
None
LAMP1-eGFP
FLAG
overlay
A
C
I
Δ
10 μm
2 μm

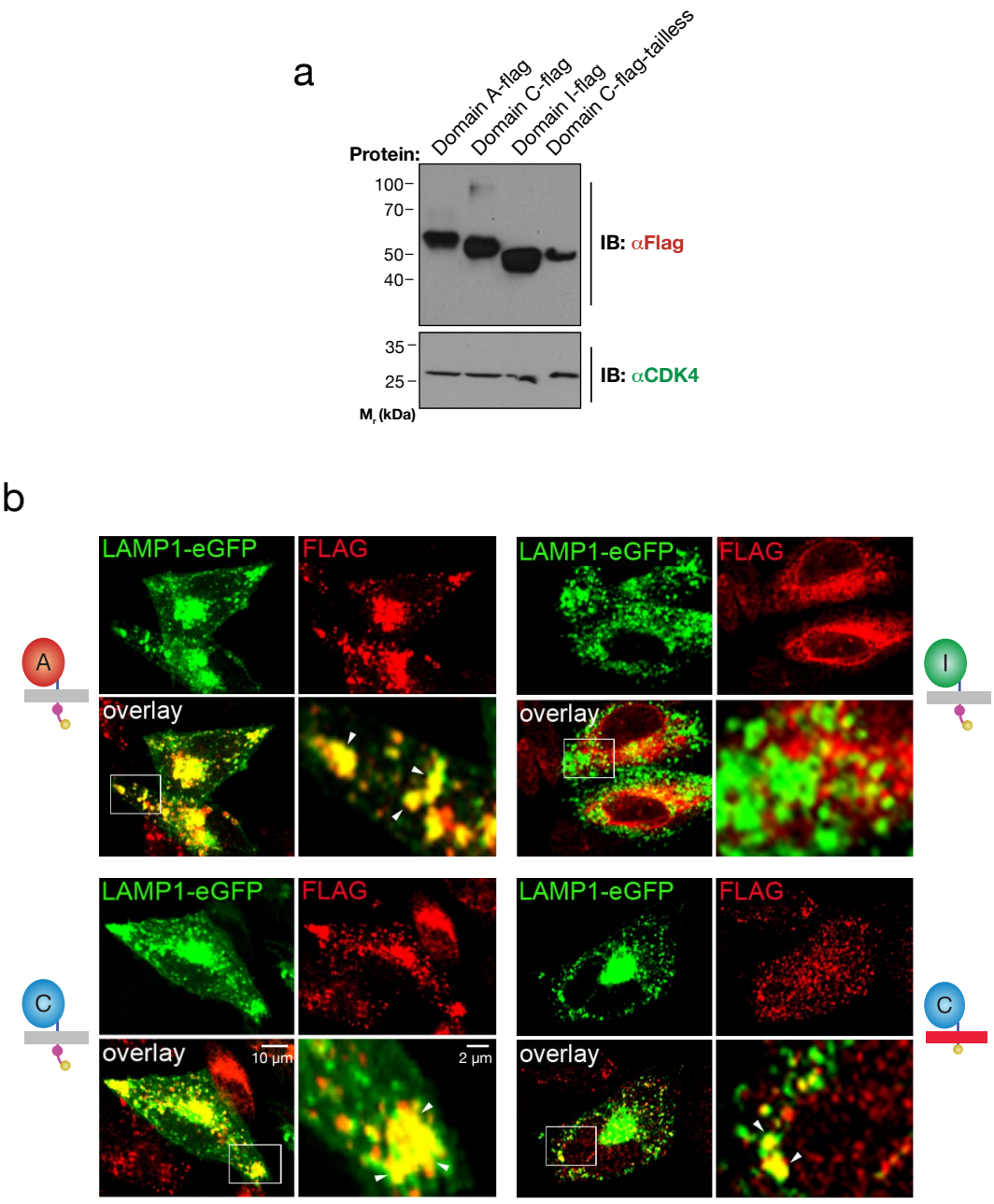
a
Domain A-flag
Domain C-flag
Domain I-flag
Domain C-flag-tailless
Protein:
100
70
50
40
IB: αFlag
35
25
IB: αCDK4
M, (kDa)
b
LAMP1-eGFP
FLAG
overlay
A
I
C
C
10 μm
2 μm

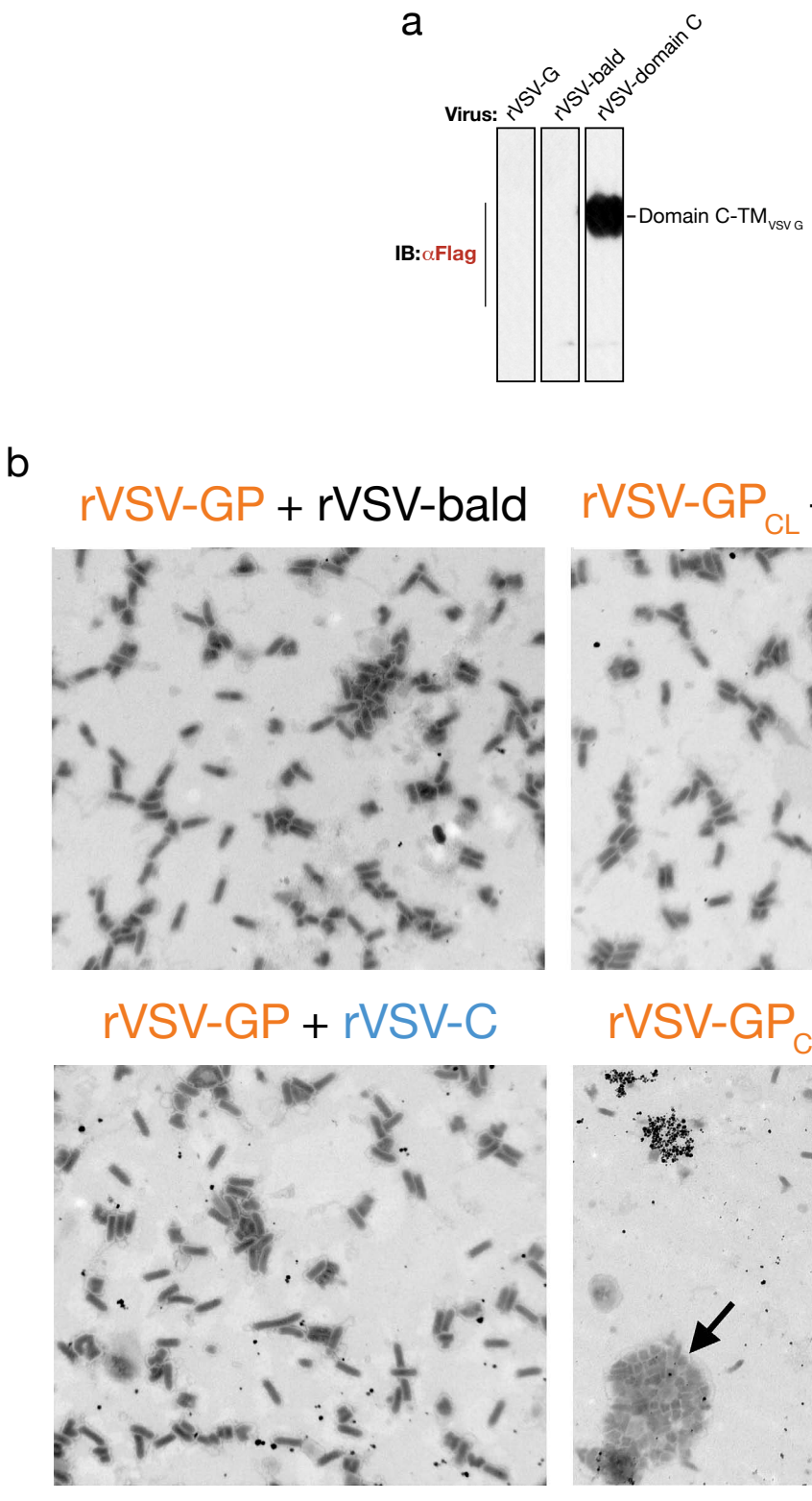
a
Virus:
rVSV-G
rVSV-bald
rVSV-domain C
IB:αFlag
Domain C-TM VSV G
b
rVSV-GP + rVSV-bald
rVSV-GP CL + rVSV-bald
rVSV-GP + rVSV-C
rVSV-GP CL + rVSV-C
500 nm

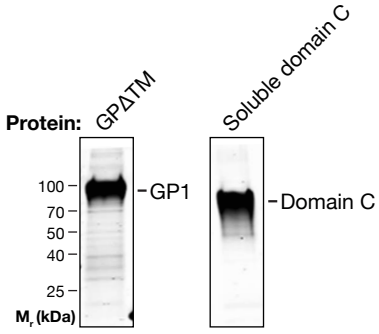
Protein:
GPΔTM
Soluble domain C
100
70
50
40
25
M, (kDa)
GP1
Domain C

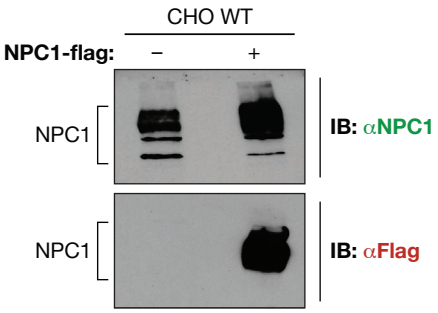
CHO WT
NPC1-flag:
–
+
NPC1
IB: αNPC1
NPC1
IB: αFlag

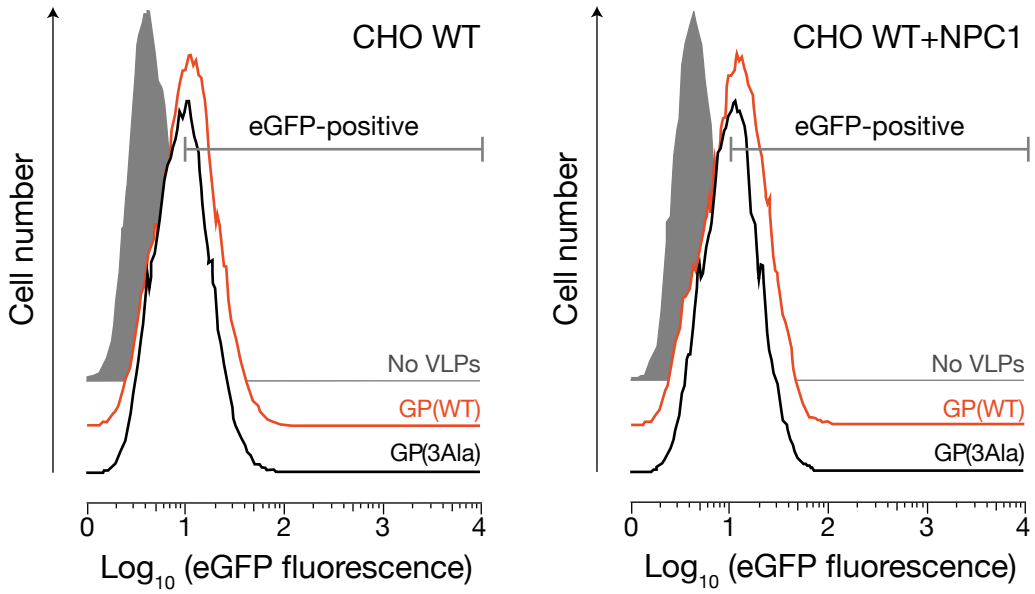
CHO WT
eGFP-positive
Cell number
No VLPs
GP(WT)
GP(3Ala)
0
1
2
3
4
Log10 (eGFP fluorescence)
CHO WT+NPC1
eGFP-positive
Cell number
No VLPs
GP(WT)
GP(3Ala)
0
1
2
3
4
Log10 (eGFP fluorescence)

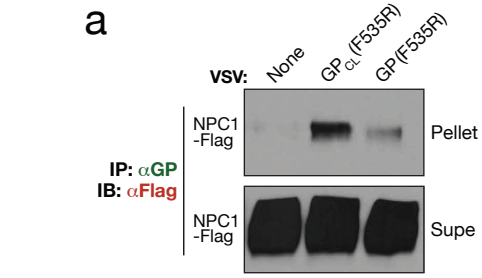
a
VSV:
None
GP CL (F535R)
GP(F535R)
IP: αGP
IB: αFlag
NPC1
-Flag
Pellet
NPC1
-Flag
Supe

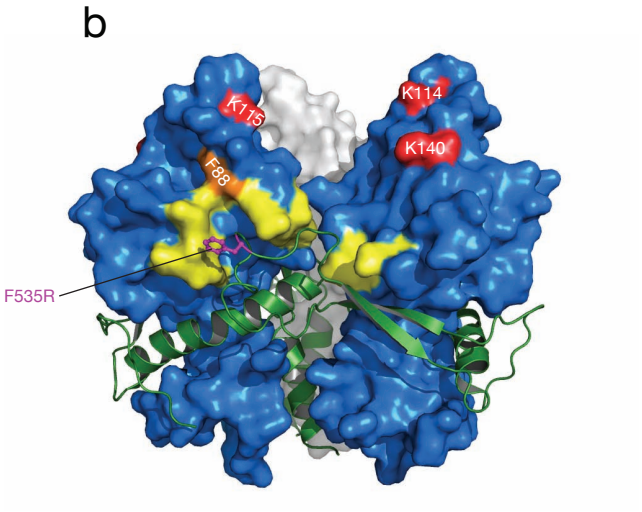
b
K115
F88
K114
K140
F535R

a

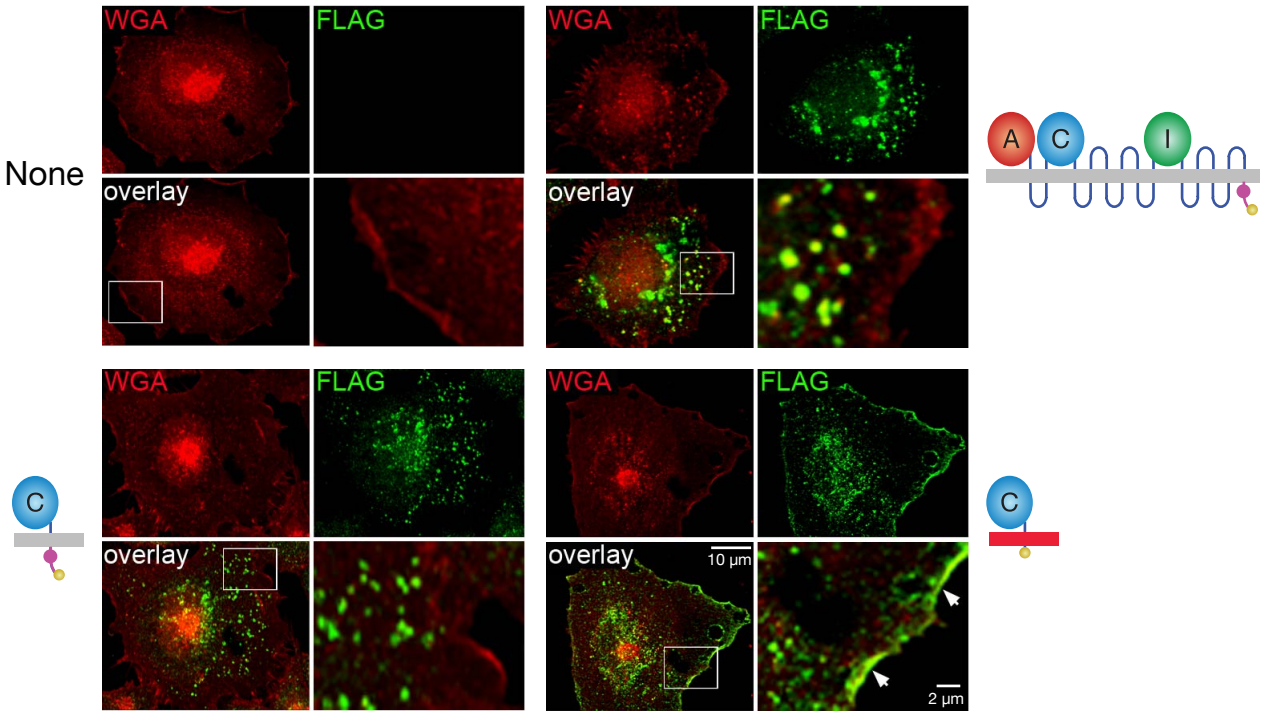
None
WGA
FLAG
overlay
A
C
I
C
10 μm
2 μm

b

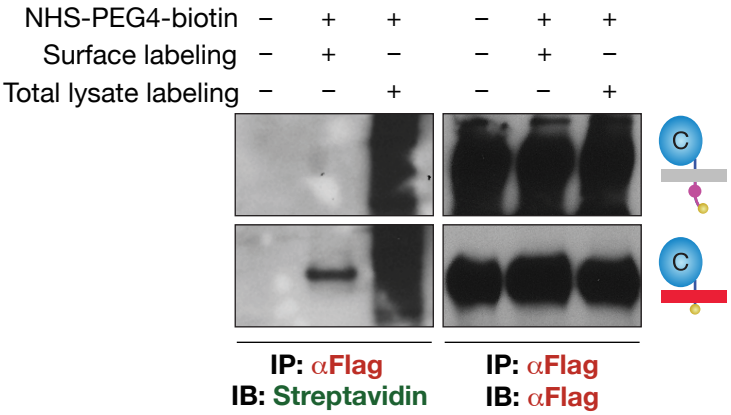
NHS-PEG4-biotin − + + − + +
Surface labeling − + − − + −
Total lysate labeling − − + − − +
C
C
IP: αFlag
IB: Streptavidin
IP: αFlag
IB: αFlag